

Implications of Cosmic Birefringence for Multi-Field ALP Dark Matter

Jialiang Shao,^{a,c} Ippei Obata,^{d,e} Dongdong Zhang^{b,1}

^aDepartment of Astronomy, School of Physical Sciences, University of Science and Technology of China, Hefei 230026, China

^bSchool of Aerospace Information, Hefei Institute of Technology, Hefei 238706, China

^cCAS Key Laboratory for Research in Galaxies and Cosmology, School of Astronomy and Space Science, University of Science and Technology of China, Hefei 230026, China

^dTheory Center, Institute of Particle and Nuclear Studies (IPNS), High Energy Accelerator Research Organization (KEK), 1-1 Oho, Tsukuba, Ibaraki 305-0801, Japan

^eKavli Institute for the Physics and Mathematics of the Universe (Kavli IPMU), WPI, UTIAS, The University of Tokyo, Kashiwa, Chiba 277-8568, Japan

E-mail: jl210898@mail.ustc.edu.cn, iohata@post.kek.jp, don@hfit.edu.cn

Abstract. Cosmic birefringence, characterized by the observed rotation of the polarization plane of the cosmic microwave background (CMB) radiation, serves as a critical probe for testing theories beyond the standard cosmological scenario. As a major component of the universe, dark matter plays a pivotal role in cosmic evolution, particularly in the formation of large-scale structures. However, its fundamental nature remains elusive. Axion-like particles (ALPs), as promising dark matter candidates, possess unique advantages in naturally explaining such phenomena. Previous studies on the implications of cosmic birefringence for these ultralight ALP fields have focused on single-field models with conventional potentials. These models face exclusion due to the washout effect—a suppression of the CMB polarization power spectrum induced by oscillatory dynamics of the scalar field within the mass range of less than 10^{-23} eV. To address this limitation, we develop a more general theoretical framework incorporating two ALP fields, providing analytical approximations and numerical calculations. Our findings reveal that the superposition of two ALP fields with distinct masses can relax the constraints imposed by the washout effect and reconcile with observations.

Keywords: Cosmic Birefringence, Axion-like Particles, Ultralight Dark Matter

¹Corresponding author

Contents

1	Introduction	1
2	Cosmic Birefringence and Axion-like Particles	2
3	Two ALP fields	5
3.1	Theoretical Model	6
3.2	Numerical Calculation	7
4	Discussion and Conclusion	9

1 Introduction

The Cosmic Microwave Background (CMB) radiation, often regarded as the afterglow of the Big Bang approximately 380,000 years after its occurrence, provides a snapshot of the baryon–photon decoupling epoch on the last scattering surface. It encodes invaluable information about the physical conditions and subsequent evolution of the early universe. In particular, studying the polarization of the CMB offers a sensitive probe of physical processes that have operated since the universe became transparent. Among these, cosmic birefringence [1–4] has recently gained considerable attention, especially given the growing need to test physics beyond the Λ CDM model.

Cosmic birefringence manifests as a rotation in the polarization direction of CMB photons during their journey from the last scattering surface to present-day observers. As a result, part of the E -mode polarization is converted into B -mode polarization, thereby mixing the E - and B -modes that would otherwise be statistically uncorrelated and generating a non-zero EB cross-power spectrum [5–11]. Such mixing serves as a sensitive diagnostic of potential parity-violating physics in the universe. Current observations of the CMB EB power spectrum have suggested a possible nonzero isotropic birefringence signal [12–17]. For instance, joint analysis of *Planck* and WMAP missions reported a polarization rotation angle $\beta = 0.34^\circ \pm 0.09^\circ$ with a 3.6σ statistical significance. Similarly, the Atacama Cosmology Telescope (ACT) Data Release (DR) 6 [18, 19] obtained $\beta = 0.215^\circ \pm 0.074^\circ$, excluding $\beta = 0$ at 2.9σ . Independent measurements, such as the POLARBEAR observations of the Crab Nebula [20], also support the existence of a time-varying birefringence signal.

To explain the measured value of isotropic cosmic birefringence, a new particle which is not included in the Standard Model is necessary [21]. Compelling theoretical interpretations of isotropic cosmic birefringence arise from the interaction between photons and axion-like particles (ALPs) as cosmological backgrounds such as dark energy [22–24], early dark energy [25–27], topological defects [28–33], or coupled to dark matter [34, 35]. The rotation angle is given by a field displacement of the ALP field between the present and the position where CMB polarization was emitted. Owing to these properties, cosmic birefringence is sensitive to the ALP dynamics starting to oscillate in the history of the universe, which enables us to conduct tomographic tests of the cosmic birefringence angle at different redshifts caused by the ALP with mass $m_\phi \lesssim 10^{-28}$ eV [36–44].

Among these parameter searches for ALPs in isotropic cosmic birefringence, its mass range over 10^{-27} eV has been less developed. For heavier mass range, the local oscillation

of ALP field at the observer’s location leads to time-dependent modulations in the observed polarization direction. Given that the oscillation period of ALP field scales inversely with its mass, for ALP mass $m_\phi \gtrsim 10^{-22}$ eV, the oscillation becomes the order of years to months comparable with the real time measurements and the birefringence angle is time-varying. Namely, a static birefringence signal requires much lighter ALPs, with $m_\phi \lesssim 10^{-22.5}$ eV. On the other hand, ALP with this mass range may experience a non-linear clustering following the gravitational instability associated with dark matter formation, and the field value can be amplified compared with the cosmological average value for $m_\phi \lesssim 10^{-28}$ eV. While it is still unclear about a transition mass scale on which non-linear clustering becomes relevant, ALP with mass beyond $m_\phi \gtrsim 10^{-25}$ eV has been confirmed to experience it from the numerical simulation of mixed fuzzy and cold dark matter system [45, 46]. Furthermore, inspired by ALPs from string theory [47–49], current cosmological observational data can be used to impose certain limitations on the mass range of axions [50]. Therefore, our analysis focuses on the mass range between 10^{-25} eV and $10^{-22.5}$ eV, where cosmic birefringence, structure formation and string theory constraints are relevant.

However, the presence of ALPs with this mass range can introduce an additional effect in the CMB polarization, the so-called washout effect [51–53]. The washout effect arises from rapid oscillations of the ALP field during the last scattering surface, which average out the rotation angle around its mean value $\bar{\beta}$ and reduce the net polarization amplitude. Recent studies [54] have shown that, under the assumption of a single ALP field, the coupling strength required to explain the observed birefringence angle is incompatible with the upper limits imposed by the washout effect for this mass range. This tension motivates the consideration of multi-field scenarios. String-inspired grand unified theories predict multiple ALP fields with independent masses and phases. Earlier works modeled their combined birefringence as a random walk, yielding a rotation angle scaling as the square root of the number of ALP fields \sqrt{N} [55, 56]. On the other hand, for the washout effect, due to its different dependence on the ALP field, an appropriate distribution of fields may lead to a different scaling behavior and potentially relax the above tension. Motivated by these considerations, this work investigates the theoretical constraints on cosmological birefringence and the washout effect within a two-field ALP framework. Through analytic and numerical calculations, we show that the superposition of multiple ALP fields with distinct masses can substantially alleviate the constraints that exclude the single-field explanation. This result opens up a broader parameter space in which ALPs remain viable candidates for the origin of cosmic birefringence.

This work is organized as follows. In Section 2, we review the theoretical basis of birefringence and the washout effect in the single-field case. In Section 3, we introduce the two-field ALP model, derive the corresponding constraints, and present our numerical results. Finally, Section 4 summarizes our findings and discusses their broader implications for ALP dark matter and parity-violating cosmology. Throughout this work, we adopt natural units with $\hbar = c = 1$.

2 Cosmic Birefringence and Axion-like Particles

In this section, we briefly review the derivation of the cosmic birefringence angle and washout effect from single ALP field dynamics. ALP field can interact with photons via a Chern-Simons term in the action:

$$S = \int d^4x \sqrt{-g} \left(-\frac{1}{2} \nabla^\mu \phi \nabla_\mu \phi - V(\phi) - \frac{1}{4} F^{\mu\nu} F_{\mu\nu} - \frac{1}{4} g_{\phi\gamma} \phi F_{\mu\nu} \tilde{F}^{\mu\nu} \right). \quad (2.1)$$

Here, ϕ denotes the ALP field, and $g_{\phi\gamma}$ represents the coupling strength between the ALP field and the electromagnetic field. This interaction breaks the symmetry between the two circular polarization modes of photons, resulting in a rotation angle β in the polarization direction of the photons. The magnitude of β depends solely on the product of the coupling constant $g_{\phi\gamma}$ and the difference in the ALP field values between the last scattering surface and the observation point:

$$\begin{aligned}\beta(\hat{n}) &= \frac{1}{2}g_{\phi\gamma}(\phi(t_0, 0) - \phi(t_{LSS}, d_{LSS}\hat{n})) \\ &= \frac{1}{2}g_{\phi\gamma}(\bar{\phi}_{obs} - \bar{\phi}_{LSS} + \delta\bar{\phi}_{obs}(\hat{n})) - \delta\bar{\phi}_{LSS}(\hat{n}) \\ &= \bar{\beta} + \delta\beta(\hat{n}),\end{aligned}\tag{2.2}$$

where t_0 is the cosmic time at the observer, \hat{n} is the unit direction vector, t_{LSS} is the cosmic time at the last scattering surface, and d_{LSS} is the comoving distance between the last scattering surface and the observer. $\bar{\beta}$ represents the isotropic component of the rotation angle, while $\delta\beta(\hat{n})$ denotes its anisotropic component which has been tightly constrained to near-zero levels by the *Planck* satellite and ground-based observatories such as BICEP, SPT and ACT missions [57–63]. When the ALP mass is less than 10^{-23} eV, the ALP de Broglie wavelength is much larger than the galactic scales, leading them to behave as wave-like dark matter. Within the Milky Way, such a field can be modeled as a wave packet composed of multiple modes with independent random phases, with the central value ϕ_0 following a Rayleigh distribution [64]:

$$P(\phi_{obs}) = \frac{2\phi_{obs}}{\phi_0^2} \exp\left(-\frac{\phi_{obs}^2}{\phi_0^2}\right).\tag{2.3}$$

Assuming that the local energy density of ALP field $\rho_{0\phi}$ contributes a fraction $\kappa_\phi \equiv \rho_{0\phi}/\rho_{0dm}$ to the local dark matter energy density near the Milky Way $\rho_{0dm} \simeq 0.4$ GeV/cm³ [65, 66], it gives:

$$\phi_0 \simeq 2.5 \times 10^{12} \text{ GeV} \times \kappa_\phi^{\frac{1}{2}} \times \left(\frac{m_\phi}{10^{-24} \text{ eV}}\right)^{-1}.\tag{2.4}$$

Since $\bar{\phi}_{obs}$ follows this Rayleigh distribution, we can place an upper bound on $\bar{\phi}_{obs}$ at the 95% confidence level as $1.73\phi_0$ [54]. In reality, the emission of CMB photons spans a finite time interval Δt_{LSS} , typically regarded as the full baryon-photon decoupling epoch, corresponding to redshifts between approximately 1200 and 1000, and a cosmic time duration of about 10^5 years. Given that $t_0 - t_{LSS} \gg \Delta t_{LSS} \gg 2\pi/m_\phi$, the axion-like field undergoes many oscillations during the photon emission period, implying $\bar{\phi}_{LSS} \approx 0$. Consequently, the rotation angle β is entirely determined by the local value of the ALP field at the observer's location. According to the latest measurements of ACT DR 6 [19], the rotation angle is given by:

$$\bar{\beta} = \frac{1}{2}g_{\phi\gamma}\phi_{obs} \simeq 0.215^\circ.\tag{2.5}$$

So, under the ALP field explanation for birefringence, the coupling constant must satisfy:

$$g_{\phi\gamma} \gtrsim 1.72 \times 10^{-15} \text{ GeV}^{-1} \times \left(\frac{m_\phi}{10^{-24} \text{ eV}}\right) \times \kappa_\phi^{-\frac{1}{2}} \times \left(\frac{\beta}{\bar{\beta}}\right).\tag{2.6}$$

However, it is essential to assess whether the associated washout effect will rule out the parameter region of cosmic birefringence or not. In an expanding universe described by the

FLRW metric $ds^2 = -dt^2 + a(t)^2 d\mathbf{x}^2$, ALP fields begin to oscillate once their mass exceeds the Hubble parameter. Under the WKB approximation, we have:

$$\phi(t) = \phi_0 a(t)^{-\frac{3}{2}} \cos(m_\phi t + \alpha(t)), \quad (2.7)$$

where $\alpha(t)$ is a phase factor which varies on the coherence time of ALP field: $\tau = 2\pi/(m_\phi v^2)$. Since CMB photons are emitted from a diffuse source randomly along the line of sight during the last scattering process, we need to evaluate the time-averaged polarization rotation induced by the oscillating ALP field at the last scattering surface, $t = t_{\text{LSS}}$. The Stokes Q and U parameters are modified as [52]:

$$(Q \pm iU)(\hat{n}) = \epsilon I e^{\pm 2i(\psi + g_{\phi\gamma}\phi(t)/2)} \langle e^{\mp ig_{\phi\gamma}\phi(t_{\text{LSS}})} \rangle, \\ \langle e^{\mp ig_{\phi\gamma}\phi(t_{\text{LSS}})} \rangle \equiv \int dt' g(t') \exp \left[\mp ig_{\phi\gamma}\phi_\star \left(\frac{1+z(t')}{1+z_\star} \right)^{3/2} \cos(m_\phi t' + \alpha(t')) \right]. \quad (2.8)$$

Here, ϵ represents the intrinsic polarization asymmetry of the source, I is the total intensity of polarization and ψ is a fixed angle between polarization detectors and CMB polarization direction without ALP coupling. The exponential term $e^{\pm ig_{\phi\gamma}\phi(t)}$ represents the local oscillation effect, arising from the oscillations of the axion field at the observer's location¹. In the time integration part, $g(t)$ is the visibility function which has a peak at around $z = 1000 - 1200$ with a time interval $\Delta t_{\text{LSS}} \sim 10^5$ yrs, and ϕ_\star denotes the field value at the central redshift of recombination epoch $z = z_\star$. As $|\partial_{t'} g(t')| \ll m_\phi$, we can divide the integration into a large number of time domains $t' \in [t'_n - \delta t'/2, t'_n + \delta t'/2]$ with $\delta t' \equiv 2\pi/m_\phi$ so that in every interval $g(t'_n) \simeq g_n$ and $z(t'_n) \simeq z_n$ can be regarded as constant. Regarding the phase factor, we can also assume a constant value $\alpha(t') \simeq \alpha'$ since the ALP coherence time scale is much longer than the time interval of last scattering surface for our interest mass range. Then, we can analytically solve it as:

$$\langle e^{\mp ig_{\phi\gamma}\phi(t_{\text{LSS}})} \rangle \simeq \sum_n g_n \int_{t'_n - \delta t'/2}^{t'_n + \delta t'/2} dt' \exp \left[\mp ig_{\phi\gamma}\phi_\star \left(\frac{1+z_n}{1+z_\star} \right)^{3/2} \cos(m_\phi t' + \alpha') \right] \\ = \sum_n g_n \delta t' J_0 \left(g_{\phi\gamma}\phi_\star \left(\frac{1+z_n}{1+z_\star} \right)^{3/2} \right) \\ = \int dt' g(t') J_0 \left(g_{\phi\gamma}\phi_\star \left(\frac{1+z(t')}{1+z_\star} \right)^{3/2} \right), \quad (2.9)$$

where we have used a formula of Bessel function: $2\pi J_0(A) = \int_{-\pi}^{\pi} dx e^{iA \cos(x+\delta)}$. Since $g(z)$ has a strong peak at $z = z_\star$, the weighted average of the ALP field amplitude in the integral is well approximated by its central value ϕ_\star in the integration. Therefore, we finally obtain the analytical formula of observed Stokes parameters:

$$(Q \pm iU)(\hat{n}) \simeq e^{\pm ig_{\phi\gamma}\phi(t)} J_0(g_{\phi\gamma}\phi_\star) (Q \pm iU)_0(\hat{n}), \quad (2.10)$$

where $(Q \pm iU)_0$ are Stokes parameters in the decoupling limit $g_{\phi\gamma} \rightarrow 0$. According to the current simulation result based on *Planck* [52], the washout effect imposes a constraint such

¹The rotation angle induced by this effect is tightly constrained by SPT-3G data; at the 95% confidence level, its impact is limited to less than 0.071° [67]. Since the local oscillation effect is based on observations made at the Earth's location, it is not subject to cosmic variance. As such, it may provide even more stringent future constraints than the washout effect [52].

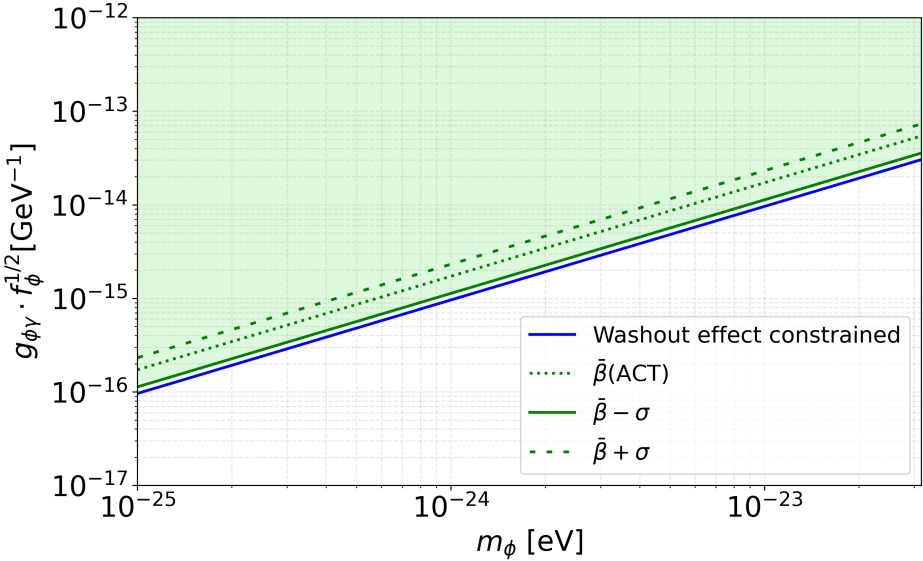


Figure 1. The constraints on the coupling constant from cosmic birefringence and Washout effect. The green area represents the coupling constant required to produce cosmic birefringence, where the solid green line, dashed line, and sparse dashed line correspond from bottom to top to different rotation angles ($\bar{\beta} = 0.215^\circ$, $\sigma = 0.074^\circ$). At the same time, the allowable parameter space should be below the blue solid line, so as not to be excluded by the Washout effect and it is easy to see that the washout effect's limitation on the coupling constant is ruled out by ACT observations within 1σ error range. In this plot, we assume that the local fraction of dark matter abundance is equal to the cosmological fraction of dark matter density: $\kappa_\phi = f_\phi$.

that, at the 95% confidence level, the reduction in polarization amplitude is limited to no more than 0.58%:

$$1 - J_0(g_{\phi\gamma}\phi_\star) \lesssim 5.8 \times 10^{-3}. \quad (2.11)$$

From the expansion $J_0(x) = 1 - x^2/4 + \mathcal{O}(x^4)$ for small x , we can see that the washout effect of ALP field exhibits a quadratic dependence on the polarization reduction, and this leads to the following upper bound on the coupling constant:

$$g_{\phi\gamma} \lesssim 9.6 \times 10^{-16} \text{ GeV}^{-1} \times \left(\frac{m_\phi}{10^{-24} \text{ eV}} \right) \times \left(f_\phi \times \frac{\Omega_{\text{DM}} h^2}{0.11933} \right)^{-\frac{1}{2}}, \quad (2.12)$$

where $f_\phi \equiv \Omega_\phi / \Omega_{\text{DM}}$ is a cosmological fraction of ALP dark matter abundance.

Regarding the formation of ALP dark matter through gravitational non-linear clustering, previous studies have shown that no significant change in the abundance fraction occurs for ALP masses $m_\phi \gtrsim 10^{-25}$ eV [45, 46]. We therefore assume $\kappa_\phi = f_\phi$ and compare the constraints in the parameter region of cosmic birefringence and the washout effect in Figure 1. It can be seen that the upper limit on the coupling constant imposed by the washout effect is approximately two times lower than the lower bound required to account for the observed cosmological birefringence. Therefore, single ALP model to explain cosmic birefringence has become less convincing.

3 Two ALP fields

In this work, we aim to perform a systematic calculation and analysis of a two-ALP field model. On one hand, we seek to resolve the issue that the coupling constant is too small to

explain the observed cosmological birefringence due to the stringent washout effect constraint. On the other hand, this study also serves as a stepping stone for exploring more natural multi-field (N -field) theories. In this section, we first derive the theoretical expressions in the two-field scenario and recalculate the conditions needed to account for the observed cosmic birefringence. We then derive approximate expressions for the washout effect, present our numerical results and compare them with constraints from the single-field scenario.

3.1 Theoretical Model

We consider a model consisting of two independently evolving ALP fields which couple to photons with the same coupling constant $g_{\phi\gamma}$. The action as follows:

$$S = \int d^4x \sqrt{-g} \left(-\frac{1}{2} \nabla^\mu \phi^1 \nabla_\mu \phi^1 - \frac{1}{2} \nabla^\mu \phi^2 \nabla_\mu \phi^2 - \frac{1}{2} m_1^2 (\phi^1)^2 - \frac{1}{2} m_2^2 (\phi^2)^2 - \frac{1}{4} F^{\mu\nu} F_{\mu\nu} - \frac{1}{4} g_{\phi\gamma} (\phi^1 + \phi^2) F_{\mu\nu} \tilde{F}^{\mu\nu} \right). \quad (3.1)$$

Each field evolves independently as

$$\phi^i(t) = \phi_{\text{ini}}^i a^{-3/2} \cos(m_i t + \alpha_i), \quad (3.2)$$

parameterized by the initial amplitude ϕ_{ini}^i , mass m_i and phase factor α_i ($i = 1, 2$). The amplitude of each field is characterized by its fractional contribution κ_i to the total dark matter density:

$$\phi_0^i \simeq 2.5 \times 10^{12} \text{ GeV} \times \kappa_i^{1/2} \times \left(\frac{m_i}{10^{-24} \text{ eV}} \right)^{-1}, \quad \kappa_1 + \kappa_2 = \kappa_\phi. \quad (3.3)$$

Substituting $\phi_{\text{obs}}^{\text{total}} = \phi_{\text{obs}}^1 + \phi_{\text{obs}}^2$ into the earlier analysis, the lowest bound on the coupling constant is obtained in the case where two ALP fields have maximum values with a same sign:

$$\begin{aligned} g_{\phi\gamma} &\gtrsim 1.72 \times 10^{-15} \text{ GeV}^{-1} \times \left(\kappa_1^{1/2} \left(\frac{m_1}{10^{-24} \text{ eV}} \right)^{-1} + \kappa_2^{1/2} \left(\frac{m_2}{10^{-24} \text{ eV}} \right)^{-1} \right)^{-1} \times \left(\frac{\beta}{0.215^\circ} \right) \\ &= 1.22 \times 10^{-15} \text{ GeV}^{-1} \times \frac{2m_1 m_2}{(m_1 + m_2) \times 10^{-24} \text{ eV}} \times \kappa_\phi^{-\frac{1}{2}} \times \left(\frac{\beta}{0.215^\circ} \right), \quad \text{for } \kappa_1 = \kappa_2. \end{aligned} \quad (3.4)$$

Here we specifically pointed out the case where κ_1 and κ_2 are equal, meaning each field occupies the same proportion of components. In principle, when one of κ_1 or κ_2 approaches 1, the two-field situation should revert to a single-field situation.

To compute the washout effect in the two-field model, the previous formula (2.9) is not strictly applicable, as it requires tracking the evolution of the multiple oscillation phases over

time. We can write the expression as:

$$\begin{aligned}
(Q \pm iU)(\hat{n}) &= \epsilon I e^{\pm 2i(\psi + g_{\phi\gamma}(\phi^1(t) + \phi^2(t))/2)} \langle e^{\mp ig_{\phi\gamma}(\phi^1(t_{\text{LSS}}) + \phi^2(t_{\text{LSS}}))} \rangle , \\
\langle e^{\mp ig_{\phi\gamma}(\phi^1(t_{\text{LSS}}) + \phi^2(t_{\text{LSS}}))} \rangle &\equiv \int dt' g(t') \exp \left[\mp ig_{\phi\gamma} \left(\frac{1+z(t')}{1+z_*} \right)^{3/2} (\phi_*^1 \cos(m_1 t' + \alpha'_1) + \phi_*^2 \cos(m_2 t' + \alpha'_2)) \right] \\
&= \int dt' g(t') \sum_{n=-\infty}^{\infty} \sum_{m=-\infty}^{\infty} (\mp i)^{n+m} \\
&\times J_n \left[g_{\phi\gamma} \phi_*^1 \left(\frac{1+z(t')}{1+z_*} \right)^{3/2} \right] J_m \left[g_{\phi\gamma} \phi_*^2 \left(\frac{1+z(t')}{1+z_*} \right)^{3/2} \right] e^{i((n m_1 + m m_2)t' + n\alpha'_1 + m\alpha'_2)} , \quad (3.5)
\end{aligned}$$

where we have used Jacobi-Anger identity $e^{\pm iA \cos \theta} = \sum_{n=-\infty}^{\infty} (\pm i)^n J_n(A) e^{in\theta}$. Since $g_{\phi\gamma}\phi^i \ll 1$, we can expand the Bessel function and keep the lowest order of $g_{\phi\gamma}\phi^i$. Then, due to a rapid oscillation of ALP field in the phase sector with $nm_1 + mm_2 \neq 0$, only the contribution from J_0 remains in the integration:

$$\begin{aligned}
\langle e^{\mp ig_{\phi\gamma}(\phi^1(t_{\text{LSS}}) + \phi^2(t_{\text{LSS}}))} \rangle &\simeq \int dt' g(t') J_0 \left[g_{\phi\gamma} \phi_*^1 \left(\frac{1+z(t')}{1+z_*} \right)^{3/2} \right] J_0 \left[g_{\phi\gamma} \phi_*^2 \left(\frac{1+z(t')}{1+z_*} \right)^{3/2} \right] \\
&\simeq J_0(g_{\phi\gamma}\phi_*^1) J_0(g_{\phi\gamma}\phi_*^2) . \quad (3.6)
\end{aligned}$$

Finally, the observed Stokes parameters are approximately given by

$$(Q \pm iU)(\hat{n}) \simeq e^{\pm ig_{\phi\gamma}(\phi^1(t) + \phi^2(t))} J_0(g_{\phi\gamma}\phi_*^1) J_0(g_{\phi\gamma}\phi_*^2) (Q \pm iU)_0(\hat{n}) . \quad (3.7)$$

Following (2.11), the constraint on the washout effect from two ALP fields reads

$$1 - J_0(g_{\phi\gamma}\phi_*^1) J_0(g_{\phi\gamma}\phi_*^2) \simeq \frac{g_{\phi\gamma}^2}{2} \left(\frac{f_1}{m_1^2} + \frac{f_2}{m_2^2} \right) \rho_{\star\text{DM}} \lesssim 5.8 \times 10^{-3} , \quad f_1 + f_2 = f_\phi . \quad (3.8)$$

This leads to the following upper bound on the coupling constant:

$$g_{\phi\gamma} \lesssim 9.6 \times 10^{-16} \text{ GeV}^{-1} \times \left(\frac{m_1 m_2}{\sqrt{f_1 m_2^2 + f_2 m_1^2}} \right) \times \frac{1}{10^{-24} \text{ eV}} \times \left(\frac{\Omega_{\text{DM}} h^2}{0.11933} \right)^{-\frac{1}{2}} . \quad (3.9)$$

Regarding the contribution from Bessel functions at the quadratic order of $g_{\gamma\phi}\phi$ in (3.5), we notice that another term $J_1(g_{\gamma\phi}\phi)J_{-1}(g_{\gamma\phi}\phi) = \mathcal{O}(g_{\gamma\phi}^2\phi^2)$ could remain with $(m_1 - m_2)t' \simeq 0$. However, when the condition $|m_1 - m_2| \gg 2\pi/\Delta t_{\text{LSS}}$ is satisfied, the frequency separation between the two fields is much larger than the inverse of the duration of recombination. Since $2\pi/\Delta t_{\text{LSS}}$ is approximately on the order of 10^{-27} eV, the condition $|m_1 - m_2| \gg 2\pi/\Delta t_{\text{LSS}}$ can be satisfied in most of parameter space. As a result, the coherence between the two modes decays rapidly, allowing this term to be neglected after the integration.

3.2 Numerical Calculation

To obtain more accurate and intuitive results, we perform direct numerical integration of the full expression. According to the most stringent constraints from CMB and large-scale structure observations, ALP can constitute the entirety of dark matter only if their mass

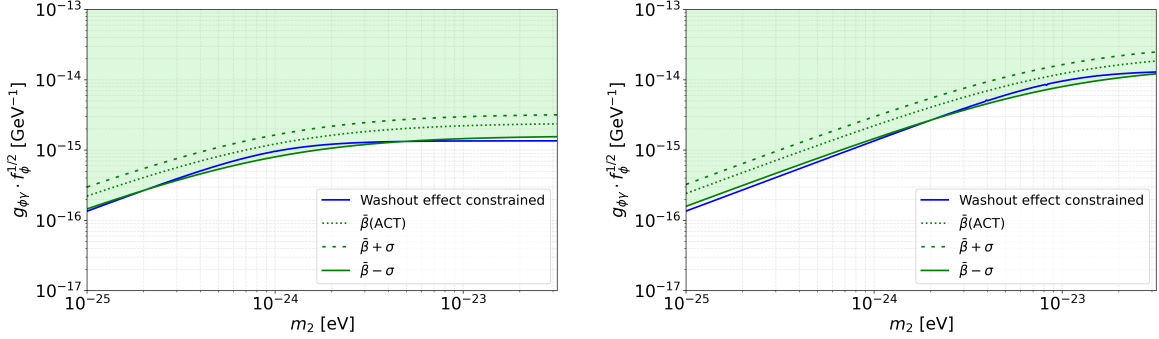


Figure 2. Constraints on the coupling constant from cosmic birefringence and the washout effect. Here $f_1 = f_2 = 0.5f_\phi$ with both ALP fields contributing equally to the total dark matter density. The panels correspond to $m_1 = 10^{-24}$ eV and $m_1 = 10^{-23}$ eV from left to right, respectively. The horizontal axis represents m_2 . The green region indicates the coupling strength required to reproduce the observed cosmic birefringence, where the solid, dashed, and sparsely dashed lines correspond (from bottom to top) to different rotation angles ($\bar{\beta} = 0.215^\circ, \sigma = 0.074^\circ$). The solid blue line denotes the limit imposed by the washout effect. When the two masses are comparable, the two-field model yields a parameter space consistent with observations within 1σ .

exceeds 10^{-24} eV. Otherwise, they can contribute only a fraction of the total dark matter density [68–71]. More recently, measurements of the UV luminosity functions of high-redshift galaxies have constrained the fractional contribution of ultra-light ALPs with masses in the range 10^{-25} eV– $10^{-22.5}$ eV to about 1% of the total dark matter [72]. In this work, we assume that the ALP fields constitute 1% of the total dark matter energy density $f_\phi = 0.01$. If we can assume $\kappa_i = f_i$ and hence $\kappa_\phi = f_\phi$, since both cosmic birefringence and the washout effect depend on f_ϕ in the same manner, varying f_ϕ does not qualitatively alter our results. For the visibility function $g(t(z))$, we adopt a Gaussian profile centered at redshift $z = 1089$. Then, choosing the span of redshift $z_{\text{span}} = 60$ ensures that $g(t)$ evolves slowly over the relevant timescale.

In Figure 2, we fix the mass of one ALP field ϕ^1 and show the parameter constraints when the two fields contribute equally to the dark matter density. The two-field model admits a more relaxed parameter space relative to the single-field case: the ratio of tension is reduced roughly by a factor of $\sqrt{2}$ around $m_1 \sim m_2$, remaining consistent with observations within the 1σ uncertainty. On the other hand, when the mass difference becomes too large, the washout effect is dominated by the lighter field, and the two-field model effectively reproduces the single-field result, which is excluded observationally.

We further consider scenarios in which the two fields contribute unequally to the dark matter density in Figure 3. When the fraction associated with the m_1 field decreases, a viable parameter region remains within the 1σ uncertainty. However, for fixed m_1 , the allowed region shifts toward larger masses. In the extreme limit where the m_1 field contributes much less than the m_2 field, the two-field model is excluded by the washout effect within 1σ across the entire mass range. In this case, the behavior effectively reduces to that of the single-field scenario.

To ensure the robustness of our conclusions, we also incorporate the constraints from WMAP and *Planck* measurements of CMB polarization [73]. Specifically, we use the combined *Planck* HFI + LFI + WMAP data, including the filamentary dust *EB* model and allowing nonzero calibration angle offsets. In this case, the observed rotation angle is $\beta = 0.34^\circ \pm 0.09^\circ$. In Figure 4, while the two-field model does not fully account for the observed

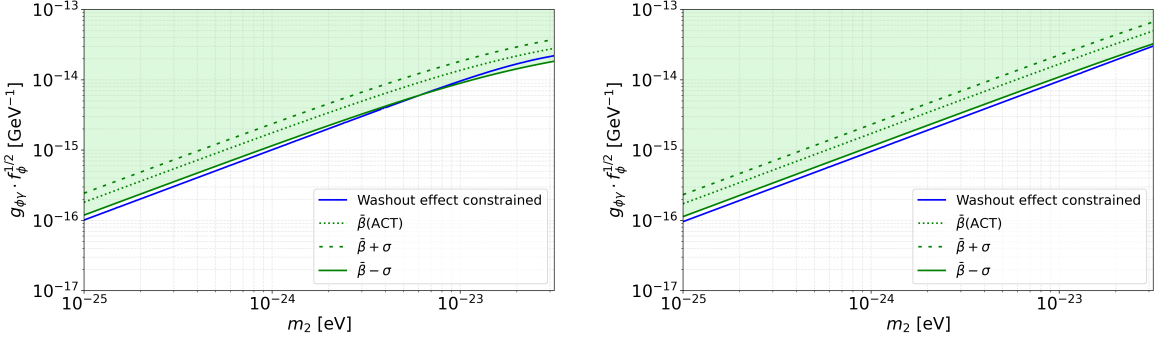


Figure 3. Constraints with $m_1 = 10^{-23}$ eV but with different f_1 and f_2 . In left panel, $f_1 = 0.1f_\phi$, $f_2 = 0.9f_\phi$. A viable parameter region consistent with observations within 1σ still exists, but shifts toward larger masses. For extreme case (right panel) with $f_1 = 0.001f_\phi$, $f_2 = 0.999f_\phi$, across the entire mass range of interest, the two-field model is excluded by the washout effect within 1σ , effectively corresponding to the single-field prediction.

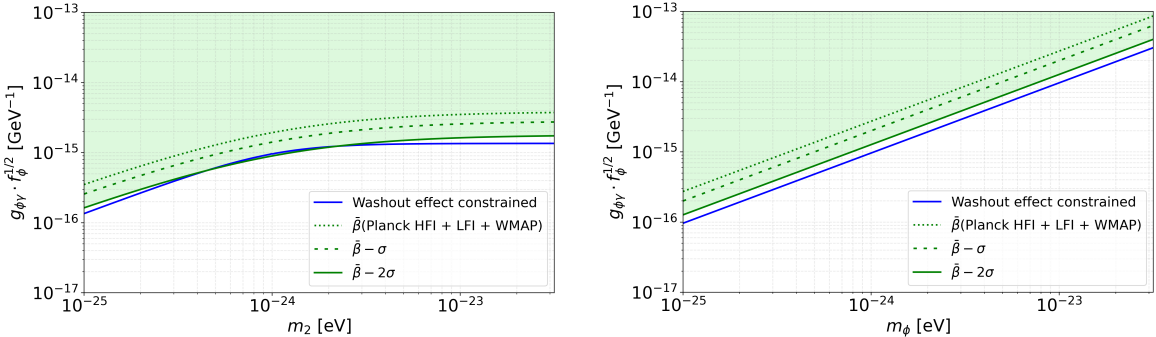


Figure 4. Constraints from the combined Planck HFI + LFI + WMAP data. The left panel shows the two-field model with $f_1 = f_2 = 0.5f_\phi$ and $m_1 = 10^{-24}$ eV, while the right panel displays the corresponding single-field case. While the two-field model does not fully account for the observed static cosmic birefringence within the 2σ constraints from Planck HFI + LFI + WMAP, it nevertheless provides a better fit than the single-field model.

static cosmic birefringence within the 2σ constraints from the data, the tension gets more relaxed than the single-field model. However, our determination of the coupling constant depends on the local dark matter density. Taking into account the uncertainties in measurements of the local dark matter density, arising from data limitations, the assumption of a flat rotation curve, or possible disequilibrium effects [74], we find that the two-field theory remains compatible with the Planck joint data at the 2σ level.

4 Discussion and Conclusion

We first briefly review the phenomenon of cosmic birefringence and proposal that ALP could potentially account for the observed effect for its masses $m_\phi \gtrsim 10^{-25}$ eV where ALP could behave as fuzzy dark matter. However, the introduction of such ALPs inevitably induces additional physical effects on the CMB polarization, namely the washout effect. We recall that, under these new constraints, the coupling strength permitted by single-field ALP models is insufficient to reproduce the observed static cosmic birefringence. Consequently, such models are ruled out by current observational data. This naturally raises the question of whether

introducing two or more ALP fields could alleviate or even resolve the difficulties encountered in the single-field scenario.

We then derive a semi-analytical expression for the upper bound on the interaction coupling constant in the two-field framework and find that the constraint primarily depends on two key factors. The first factor is the mass hierarchy between the two fields. When the mass difference between the two fields becomes too large, the washout effect is dominated by the lighter field, causing the two-field scenario to effectively reduce to the single-field case, which is then excluded by observations. When masses are comparable, the constraint from washout effect have been relaxed, alleviating the tension by 1σ compared to a single field case. The second factor is the fraction hierarchy. Once the fraction of one field falls below 0.1%, two-field model will obtain similar constraint results to the single-field model. We further present numerical results and compare them with the single-field constraint curves to verify the validity of our theoretical estimates. Our findings indicate that the two-field model can indeed relax the washout effect constraints and explain the cosmic birefringence signal from ACT DR6 and potentially from *Planck*/WMAP data.

We can now assume a simple case for the extension to N fields, where each field occupies the same order of component, initial phases and masses. In this case, explaining cosmic birefringence, within the limits allowed by washout effect, would roughly require $\sqrt{N} \gtrsim 3$. More dedicated search for the probability distribution of parameter space leaves in our future work. Our calculations also rely on measurements of the dark matter density at the observer's location. If ALPs could constitute a higher proportion of the dark matter in the solar system [75, 76], then the number of ALP fields needed to explain cosmic birefringence would decrease accordingly.

Acknowledgments

We are grateful for Yi-Fu Cai, Elisa Ferreira, Kai Murai and Fumihiro Naokawa for insightful discussions. This work is supported in part by the Hefei Institute of Technology Talent Research Fund (2025KY41), by the National Key R&D Program of China (2021YFC2203100, 2024YFC2207500), by the National Natural Science Foundation of China (12433002, 12261131497, 92476203), by CAS young interdisciplinary innovation team (JCTD-2022-20), by 111 Project (B23042), by USTC Fellowship for International Cooperation, by USTC Research Funds of the Double First-Class Initiative and by JSPS KAKENHI Grant No. 19K14702 (IO).

References

- [1] S. M. Carroll, G. B. Field, and R. Jackiw, [Phys. Rev. D **41**, 1231 \(1990\)](#).
- [2] S. M. Carroll and G. B. Field, [Phys. Rev. D **43**, 3789 \(1991\)](#).
- [3] D. Harari and P. Sikivie, [Phys. Lett. B **289**, 67 \(1992\)](#).
- [4] B. Nodland and J. P. Ralston, [Phys. Rev. Lett. **78**, 3043 \(1997\)](#), [arXiv:astro-ph/9704196](#) .
- [5] A. Lue, L.-M. Wang, and M. Kamionkowski, [Phys. Rev. Lett. **83**, 1506 \(1999\)](#), [arXiv:astro-ph/9812088](#) .
- [6] B. Feng, M. Li, J.-Q. Xia, X. Chen, and X. Zhang, [Phys. Rev. Lett. **96**, 221302 \(2006\)](#), [arXiv:astro-ph/0601095](#) .
- [7] M. Pospelov, A. Ritz, and C. Skordis, [Phys. Rev. Lett. **103**, 051302 \(2009\)](#).
- [8] S. Lee, G.-C. Liu, and K.-W. Ng, [Phys. Rev. D **89**, 063010 \(2014\)](#).

- [9] W. Zhao and M. Li, [Phys. Rev. D](#) **89**, 103518 (2014).
- [10] P. D. Lasky *et al.*, [Phys. Rev. X](#) **6**, 011035 (2016), arXiv:1511.05994 [astro-ph.CO] .
- [11] G.-B. Zhao, Y. Wang, J.-Q. Xia, M. Li, and X. Zhang, [JCAP](#) **07**, 032 (2015), arXiv:1504.04507 [astro-ph.CO] .
- [12] Y. Minami and E. Komatsu, [Physical Review Letters](#) **125** (2020), 10.1103/physrevlett.125.221301.
- [13] P. Diego-Palazuelos *et al.*, [Phys. Rev. Lett.](#) **128**, 091302 (2022), arXiv:2201.07682 [astro-ph.CO] .
- [14] J. R. Eskilt, [Astronomy & Astrophysics](#) **662**, A10 (2022).
- [15] J. R. Eskilt and E. Komatsu, [Physical Review D](#) **106** (2022), 10.1103/physrevd.106.063503.
- [16] J. R. Eskilt *et al.* (Cosmoglobe), [Astron. Astrophys.](#) **679**, A144 (2023), arXiv:2305.02268 [astro-ph.CO] .
- [17] E. Komatsu, [Nature Reviews Physics](#) **4**, 452–469 (2022).
- [18] T. Louis *et al.* (Atacama Cosmology Telescope), [JCAP](#) **11**, 062 (2025), arXiv:2503.14452 [astro-ph.CO] .
- [19] P. Diego-Palazuelos and E. Komatsu, (2025), arXiv:2509.13654 [astro-ph.CO] .
- [20] S. Adachi *et al.* (POLARBEAR), [Phys. Rev. D](#) **110**, 063013 (2024), arXiv:2403.02096 [astro-ph.CO] .
- [21] Y. Nakai, R. Namba, I. Obata, Y.-C. Qiu, and R. Saito, [JHEP](#) **01**, 057 (2024), arXiv:2310.09152 [astro-ph.CO] .
- [22] T. Fujita, Y. Minami, K. Murai, and H. Nakatsuka, [Phys. Rev. D](#) **103**, 063508 (2021), arXiv:2008.02473 [astro-ph.CO] .
- [23] G. Choi, W. Lin, L. Visinelli, and T. T. Yanagida, [Phys. Rev. D](#) **104**, L101302 (2021), arXiv:2106.12602 [hep-ph] .
- [24] S. Gasparotto and I. Obata, [JCAP](#) **08**, 025 (2022), arXiv:2203.09409 [astro-ph.CO] .
- [25] T. Fujita, K. Murai, H. Nakatsuka, and S. Tsujikawa, [Phys. Rev. D](#) **103**, 043509 (2021), arXiv:2011.11894 [astro-ph.CO] .
- [26] K. Murai, F. Naokawa, T. Namikawa, and E. Komatsu, [Phys. Rev. D](#) **107**, L041302 (2023), arXiv:2209.07804 [astro-ph.CO] .
- [27] J. R. Eskilt, L. Herold, E. Komatsu, K. Murai, T. Namikawa, and F. Naokawa, [Phys. Rev. Lett.](#) **131**, 121001 (2023), arXiv:2303.15369 [astro-ph.CO] .
- [28] F. Takahashi and W. Yin, [JCAP](#) **04**, 007 (2021), arXiv:2012.11576 [hep-ph] .
- [29] N. Kitajima, F. Kozai, F. Takahashi, and W. Yin, [JCAP](#) **10**, 043 (2022), arXiv:2205.05083 [astro-ph.CO] .
- [30] D. Gonzalez, N. Kitajima, F. Takahashi, and W. Yin, [Phys. Lett. B](#) **843**, 137990 (2023), arXiv:2211.06849 [hep-ph] .
- [31] R. Z. Ferreira, S. Gasparotto, T. Hiramatsu, I. Obata, and O. Pujolas, [JCAP](#) **05**, 066 (2024), arXiv:2312.14104 [hep-ph] .
- [32] M. Jain, A. J. Long, and M. A. Amin, [JCAP](#) **05**, 055 (2021), arXiv:2103.10962 [astro-ph.CO] .
- [33] M. Jain, R. Hagimoto, A. J. Long, and M. A. Amin, [JCAP](#) **10**, 090 (2022), arXiv:2208.08391 [astro-ph.CO] .
- [34] S. Nakagawa, F. Takahashi, and M. Yamada, [Phys. Rev. Lett.](#) **127**, 181103 (2021), arXiv:2103.08153 [hep-ph] .

- [35] I. Obata, [JCAP **09**, 062 \(2022\)](#), arXiv:2108.02150 [astro-ph.CO] .
- [36] B. D. Sherwin and T. Namikawa, [Mon. Not. Roy. Astron. Soc. **520**, 3298 \(2023\)](#), arXiv:2108.09287 [astro-ph.CO] .
- [37] H. Nakatsuka, T. Namikawa, and E. Komatsu, [Phys. Rev. D **105**, 123509 \(2022\)](#), arXiv:2203.08560 [astro-ph.CO] .
- [38] T. Namikawa, K. Murai, and F. Naokawa, [Phys. Rev. D **112**, 123513 \(2025\)](#), arXiv:2506.20824 [astro-ph.CO] .
- [39] N. Lee, S. C. Hotinli, and M. Kamionkowski, [Phys. Rev. D **106**, 083518 \(2022\)](#), arXiv:2207.05687 [astro-ph.CO] .
- [40] T. Namikawa and I. Obata, [Phys. Rev. D **108**, 083510 \(2023\)](#), arXiv:2306.08875 [astro-ph.CO] .
- [41] F. Naokawa and T. Namikawa, [Phys. Rev. D **108**, 063525 \(2023\)](#), arXiv:2305.13976 [astro-ph.CO] .
- [42] W. W. Yin, L. Dai, J. Huang, L. Ji, and S. Ferraro, [Phys. Rev. Lett. **134**, 161001 \(2025\)](#), arXiv:2402.18568 [astro-ph.CO] .
- [43] F. Naokawa, (2025), arXiv:2504.06709 [astro-ph.CO] .
- [44] F. Naokawa, T. Namikawa, K. Murai, I. Obata, and K. Kamada, (2024), arXiv:2405.15538 [astro-ph.CO] .
- [45] B. Schwabe, M. Gosenca, C. Behrens, J. C. Niemeyer, and R. Easther, [Phys. Rev. D **102**, 083518 \(2020\)](#), arXiv:2007.08256 [astro-ph.CO] .
- [46] A. Laguë, B. Schwabe, R. Hložek, D. J. E. Marsh, and K. K. Rogers, [Phys. Rev. D **109**, 043507 \(2024\)](#), arXiv:2310.20000 [astro-ph.CO] .
- [47] P. Svrcek and E. Witten, [Journal of High Energy Physics **2006**, 051–051 \(2006\)](#).
- [48] J. P. Conlon, [Journal of High Energy Physics **2006**, 078–078 \(2006\)](#).
- [49] A. Arvanitaki, S. Dimopoulos, S. Dubovsky, N. Kaloper, and J. March-Russell, [Phys. Rev. D **81**, 123530 \(2010\)](#), arXiv:0905.4720 [hep-th] .
- [50] L. Visinelli and S. Vagnozzi, [Phys. Rev. D **99**, 063517 \(2019\)](#).
- [51] F. Finelli and M. Galaverni, [Phys. Rev. D **79**, 063002 \(2009\)](#).
- [52] M. A. Fedderke, P. W. Graham, and S. Rajendran, [Phys. Rev. D **100**, 015040 \(2019\)](#).
- [53] K. Murai, [Phys. Rev. D **111**, 043514 \(2025\)](#).
- [54] D. Zhang, E. G. M. Ferreira, I. Obata, and T. Namikawa, [Phys. Rev. D **110**, 103525 \(2024\)](#), arXiv:2408.08063 [astro-ph.CO] .
- [55] S. Gasparotto and E. I. Sfakianakis, [JCAP **11**, 017 \(2023\)](#), arXiv:2306.16355 [astro-ph.CO] .
- [56] N. Gendler, D. J. E. Marsh, L. McAllister, and J. Moritz, [JCAP **09**, 071 \(2024\)](#), arXiv:2309.13145 [hep-th] .
- [57] P. A. R. Ade *et al.* (BICEP2, Keck Array), [Phys. Rev. D **96**, 102003 \(2017\)](#), arXiv:1705.02523 [astro-ph.CO] .
- [58] P. A. R. Ade *et al.* (BICEP/Keck), [Astrophys. J. **949**, 43 \(2023\)](#), arXiv:2210.08038 [astro-ph.CO] .
- [59] T. Namikawa *et al.*, [Phys. Rev. D **101**, 083527 \(2020\)](#), arXiv:2001.10465 [astro-ph.CO] .
- [60] F. Bianchini *et al.* (SPT), [Phys. Rev. D **102**, 083504 \(2020\)](#), arXiv:2006.08061 [astro-ph.CO] .
- [61] M. Bortolami, M. Billi, A. Gruppuso, P. Natoli, and L. Pagano, [JCAP **09**, 075 \(2022\)](#), arXiv:2206.01635 [astro-ph.CO] .

- [62] G. Zagatti, M. Bortolami, A. Gruppuso, P. Natoli, L. Pagano, and G. Fabbian, *JCAP* **05**, 034 (2024), arXiv:2401.11973 [astro-ph.CO] .
- [63] T. Namikawa, *Phys. Rev. D* **109**, 123521 (2024), arXiv:2404.13771 [astro-ph.CO] .
- [64] G. P. Centers *et al.*, *Nature Commun.* **12**, 7321 (2021), arXiv:1905.13650 [astro-ph.CO] .
- [65] F. Iocco, M. Pato, and G. Bertone, *Nature Physics* **11**, 245–248 (2015).
- [66] S. Sivertsson, H. Silverwood, J. I. Read, G. Bertone, and P. Steger, *Monthly Notices of the Royal Astronomical Society* **478**, 1677–1693 (2018).
- [67] K. R. Ferguson *et al.* (SPT-3G), *Phys. Rev. D* **106**, 042011 (2022), arXiv:2203.16567 [astro-ph.CO] .
- [68] R. Hložek, D. Grin, D. J. Marsh, and P. G. Ferreira, *Physical Review D* **91** (2015), 10.1103/physrevd.91.103512.
- [69] R. Hložek, D. J. E. Marsh, and D. Grin, *Monthly Notices of the Royal Astronomical Society* **476**, 3063–3085 (2018).
- [70] A. Laguë, J. Bond, R. Hložek, K. Rogers, D. Marsh, and D. Grin, *Journal of Cosmology and Astroparticle Physics* **2022**, 049 (2022).
- [71] K. K. Rogers, R. Hložek, A. Laguë, M. M. Ivanov, O. H. Philcox, G. Cabass, K. Akitsu, and D. J. Marsh, *Journal of Cosmology and Astroparticle Physics* **2023**, 023 (2023).
- [72] H. Winch, K. K. Rogers, R. Hložek, and D. J. E. Marsh, *Astrophys. J.* **976**, 40 (2024), arXiv:2404.11071 [astro-ph.CO] .
- [73] J. R. Eskilt and E. Komatsu, *Phys. Rev. D* **106**, 063503 (2022), arXiv:2205.13962 [astro-ph.CO] .
- [74] S. Sivertsson, H. Silverwood, J. I. Read, G. Bertone, and P. Steger, *Mon. Not. Roy. Astron. Soc.* **478**, 1677 (2018), arXiv:1708.07836 [astro-ph.GA] .
- [75] M. Cuadrat-Grzybowski, S. Clesse, P. Defraigne, M. Van Camp, and B. Bertrand, *Phys. Rev. D* **110**, 063029 (2024), arXiv:2403.14397 [astro-ph.CO] .
- [76] D. Budker, J. Eby, M. Gorghetto, M. Jiang, and G. Perez, *JCAP* **12**, 021 (2023), arXiv:2306.12477 [hep-ph] .